YbGG material for Adiabatic Demagnetization in the 100 mK–3 K range

Diego Augusto Paixao Brasiliano, Jean-Marc Duval, Christophe Marin, Emmanuelle Bichaud, Jean-Pascal Brison, Mike Zhitomirsky, Nicolas Luchier

Version of Record: https://www.sciencedirect.com/science/article/pii/S0011227519302413
Manuscript_7f600fb7846ac483d5a247c988a0bbf7

YbGG material for Adiabatic Demagnetization in the 100 mK – 3 K range

Abstract

Adiabatic Demagnetization Refrigerators (ADR) are particularly well adapted for the lowest temperature cooling requirements of the recent and planned astrophysics missions, such as Hitomi, Athena, SPICA or LiteBIRD. With the dilution refrigerator, they are the only established technologies for space to reach temperatures below 200 mK. In the present work, we focus on the heart of the ADR, the paramagnetic material. While the efficiency of the ADR cycle at the material level is close to that of the Carnot cycle, improving the cooling output (temperature ratio or cooling power) per mass of the cooler is critical for space instruments.

In this work, we demonstrate that for ADR stages of similar size, higher cooling power or higher temperature ratios can be achieved using Ytterbium Gallium Garnet ($Yb_3Ga_5O_{12}$, YbGG), rather than more traditional materials. We have produced and characterized high-quality YbGG crystals and our results show that YbGG is particularly well suited for the 2 K – 200 mK range, providing in some cases, for the same material volume and magnetic field, a cooling capacity more than three times higher than conventional materials such as CPA.

We present the path that lead to the choice of YbGG, and our experimental results. Potential applications of this material are also discussed.

Authors list

Diego Augusto Paixao Brasiliano[1, now 2], Jean-Marc Duval[1], Christophe Marin[3], Emmanuelle Bichaud[3], Jean-Pascal Brison[3], Mike Zhitomirsky[3], Nicolas Luchier[1]

Affiliation:

[1] Univ. Grenoble Alpes, CEA, IRIG, DSBT, F-38000 Grenoble, France

[2] Univ. Grenoble Alpes, CNRS, Institut Néel, F-38000 Grenoble, France

[3] Univ. Grenoble Alpes, CEA, IRIG, PHELIQS, F-38000 Grenoble, France

Highlights

The main points of this article are:

- The description of a novel material for use in ADR: Ytterbium Gallium Garnet
- The measurements of this material's properties

Keywords

Cryocooler, Adiabatic Demagnetization Refrigerator, Magnetic material

1. Introduction

Adiabatic Demagnetization Refrigerators (ADR) are proposed for future space missions such as LiteBIRD, ATHENA or SPICA. ADR are extremely efficient at low temperature and can provide subkelvin temperatures where only few other technologies can provide this temperature level. This technology is well adapted for space use as it is insensitive to gravity and thermodynamically efficient. One of the main perturbations caused by an ADR on the highly sensitive detectors used for astrophysics missions is the changing magnetic field outside the ADR. To limit this parasitic magnetic field, a ferromagnetic shield encompasses the magnetic coil and the magnetic material. Reducing the mass of the system, originating in a large part from this ferromagnetic shield, is a strong design driver for space ADR. The mass is directly linked to the desired maximum magnetic field, the volume of the paramagnetic material and the allowed maximum stray field. To limit the mass of the system, new magnetic materials that provide larger cooling power for a given volume or magnetic field should be used. It is, however, particularly difficult to propose new materials, as on one hand the list of potential candidates is extensive and on the other hand, the manufacturing and characterization of the material is timely and costly. Finally, very efficient materials have already been proposed: for example, [Wikus et al, 2011] proposed a study of paramagnetic materials for use in ADR, and compared their properties over different temperature ranges.

Guided by theoretical inputs, we have made an intensive search for new materials, and finally, found a material with a high potential for an intermediate temperature range (typically 2 K – 200 mK) [Brasiliano, 2017]. We describe in this paper this proposed material, mostly overlooked by the community, Ytterbium Gallium Garnet (YbGG, $Yb_3Ga_5O_{12}$). One of the reasons for this disregard is that it is usually considered that materials with high J have better properties [Barclay and Steyert, 1982]. Materials with lower J, however, can have good performance if the product of their magnetic ion density and Landé g-factor is high for their ordering temperature [Brasiliano, 2017]. A list of compounds with high g-factors can be found in [Brasiliano, 2017]. They are characterized by the presence of a non-zero orbital angular momentum and are thus more affected by crystal field effects than materials with zero orbital angular momentum [Barclay and Steyert, 1982]. YbGG has been described previously in [Filippi et al, 1980]. It belongs to the class of geometrically frustrated magnets, and as such, behaves mainly as a paramagnetic material down to very low temperature despite a high density of magnetic ions [Zhitomirsky, 2003].

This paper describes the YbGG synthesis process, as well as the measurements of its magnetocaloric and thermal properties. It concludes with an example of application that highlights the advantages of using YbGG instead of more common materials.

2. Material's description and synthesis

A suitable material for space ADR is required to have a high cooling capacity per volume for a given magnetic field. This cooling capacity can be directly deduced from the entropy diagram S=S(T,B). This diagram can be obtained from a simplified theoretical model whose free parameters are fitted based on the heat capacity measurements described here. Furthermore, to be able to extract the heat, a good thermal conductivity is advantageous to avoid inefficiencies and the use of a complex thermal bus. We present in this section the characterization of YbGG required to address these points. YbGG has been intensively studied in [Filippi et al, 1980]. Its ground state has a magnetic moment J of ½ and a quasi-isotropic Landé factor of 3.43. Its specific heat exhibits a sharp peak at 54 mK and a very broad peak at 180 mK. Its general properties are summarized in table 1, which also includes the properties of a few common low temperature materials.

Table 1: Elementary characteristics of YbGG and some common magnetocaloric materials.

Material	J	Landé g-factor	Magnetic ion density (cm^3)	T_{Neel} (K)
YbGG	1/2	3.43	1.32×10^{22}	0.054
CPA	3/2	2	2.20×10^{21}	0.009
GLF	7/2	2	1.43×10^{22}	<0.25
GGG	7/2	2	1.27×10^{22}	
DGG	1/2	8	1.24×10^{22}	

Crystal growth of large Ytterbium garnets

For our first characterization, centimeter-size single crystals of YbGG were grown by the floating zone method using an optical furnace (Crystal Systems Corp. / 4 mirrors type, model FZ-T-10000-H). Feed rods were prepared by solid-state reaction from high purity starting powders Yb_2O_3 (99.99%) and Ga_2O_3 (99.99%). Isostatic pressing (250 MPa) and high temperature sintering up to 1400°C were essential to obtain high-density ceramic rods (length ~100 mm). The molten zone was stabilized through a flow of Argon gas under pressure (0.5 MPa) at a growth rate of 10 mm per hour. Typical dimensions of YbGG crystallized rods were 8 mm of diameter over several centimeters. Single crystallinity and phase purity were checked by X Ray Laue technique and X Ray powder diffraction; growth direction was found to be systematically near the (100) crystallographic axis. The magnetic properties of the single crystals were confirmed using a SQUID magnetometer (Quantum Design MPMS).

To be able to manufacture larger size pills, polycrystalline materials have also been manufactured and characterized.

Modelling the entropy value

The main property to describe the behavior of a material used in ADRs is the entropy as function of magnetic field and temperature. A simplified model for paramagnetic material is based on the free ion approximation [Pobell, 2007] and expresses the entropy as follow:

$$\frac{S}{nR} = \ln\left\{\frac{\sinh\left[\left(J+{}^{1}/_{2}\right)x\right]}{\sinh\left({}^{x}/_{2}\right)}\right\} - xB_J(x)$$

with S the entropy, n the number of moles of paramagnetic ions per mole of material, J the magnetic moment and x a dimensionless number defined as:

$$x = \frac{g\mu_B B}{kT}$$

with $\mu_B = 9.274 \times 10^{-24}$ J/T being the Bohr magneton, k $= 1.38 \times 10^{-24}$ J/K the Boltzmann constant and g the Landé factor.

The Brillouin function B_J is expressed as:

$$B_J(x) = \frac{1}{J}\left[(J + {}^1/_2)\coth[(J + {}^1/_2)x] - \frac{1}{2}\coth({}^x/_2)\right]$$

The above model fails for small values of either temperature or magnetic field, once interactions between magnetic ions become significant. With the introduction of a so-called "internal field", however, it is possible to represent better the experimental data including those conditions by replacing the value of B in the expression of x by an effective field B_{eff} defined as:

$$B^2_{eff} = B^2 + B^2_{int}$$

Values of B_{int} for common materials used in low temperature ADRs can be found in [Shirron, 2014]. Based on the data we present in this paper, we found that the following form of B_{int} proposed on the cited paper is well suited for reproducing YbGG entropy diagram.

$$B_{int} = b_0\left(1 - e^{-(T/T_0)^\alpha}\right)$$

The determination of the free parameters of B_{int} - b_0, T_0, α - that best fit our data was based on measurements of zero-field entropy and on measurements of entropy change at constant temperature.

Heat capacity measurements

Heat capacity measurements have been made on monocrystalline (using a Quantum Design PPMS) and on polycrystalline material. This last measurement was done on a full pill assembly containing 400 g (51.6 cm^3) of YbGG. The measurement on the polycrystalline material have therefore larger uncertainty (homogeneity of the applied magnetic field, thermal gradient during measurements). Figure 1 shows the results of these measurements together with the published experimental data [Filippi et al, 1980 and Onn et al, 1967]. Except for the lowest temperatures, the agreement between the monocrystalline and the polycrystalline measurements confirms that our pills do not introduce unintended heat capacity.

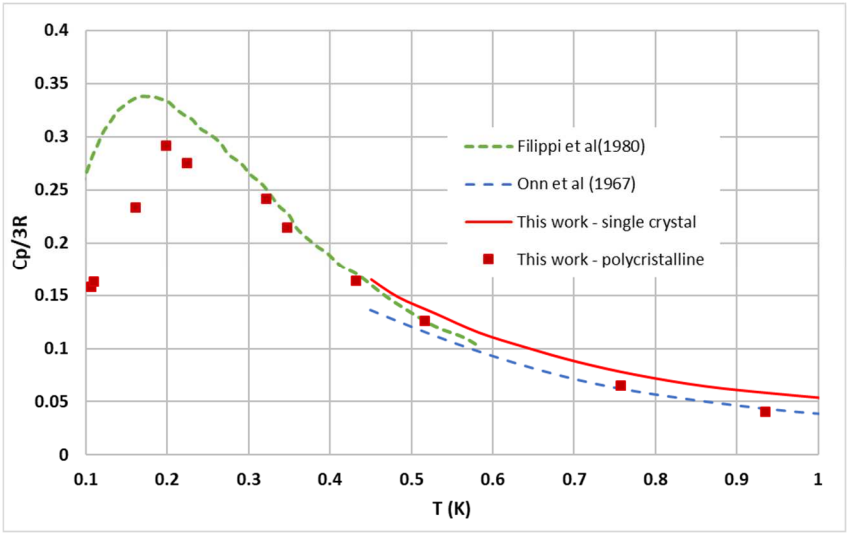

Figure 1 – Normalized heat capacity of YbGG, with data from this work and literature.

The zero field entropy S_0 calculated from the specific heat measurements of YbGG single crystal (C_P=T·dS/dT) is shown in figure 2, as well as the entropy diagram calculated with the free ion model. The values of the parameters b_0, T_0 and α of B_{int} that best fit the data are the following:

$$b_0 = 0.21\ \mathrm{T}$$
$$T_0 = 9.47 \cdot 10^{-2}\ \mathrm{K}$$
$$\alpha = 0.4287$$

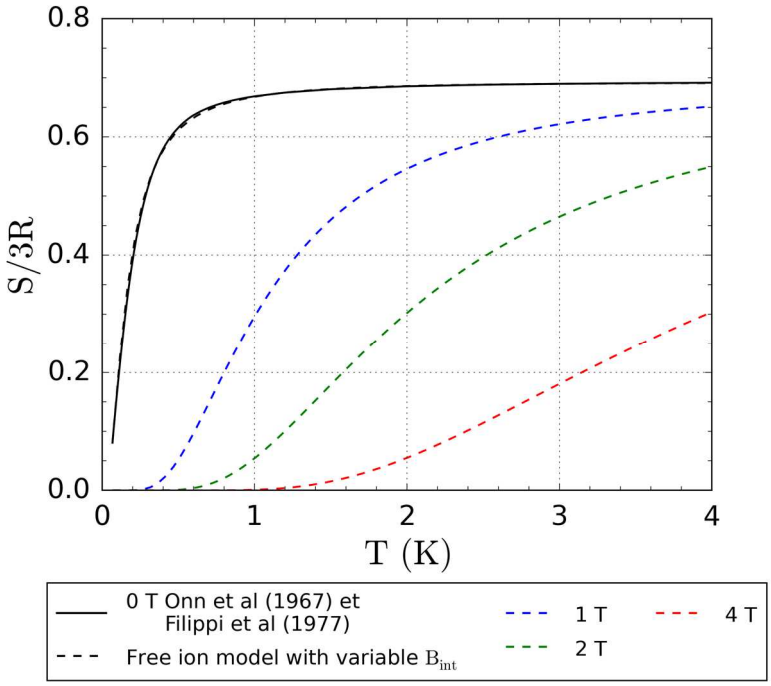

Figure 2 –Entropy diagram of YbGG. Full line corresponds to the zero field entropy obtained from specific heat measurements of single crystals. Dashed lines were calculated based on the free ion model described on the text.

Heat conductivity elementary characterization

The thermal conductivity of a paramagnetic refrigerant, combined with other factors such as the required cooling power, drives the design of the refrigerant's thermal bus. We have characterized the thermal conductivity of YbGG single and polycrystalline samples in a

dilution refrigerator with a standard one heater-two thermometers technique in order to get insights on the mechanisms controlling the value of the thermal conductivity, which may guide the efforts for improving the heat transfers on a full pill. Temperature gradients between 0.1 and 1% have been applied on bar-shaped samples, so as to have a geometrical factor defined with an accuracy of better than 10%. The (steady-state) measurements were very difficult below 0.3 K, due to diverging thermal relaxation times (8 hours required to get a reliable point at 0.1 K on the polycrystalline material). The thermal conductivity below 1 K behaves essentially as T^3, which is the hallmark of heat transport by phonons, with a mean-free path limited by the crystal size. This is consistent with the sample dependence of the results, showing that switching from polycrystals to single crystals of the same diameter increases the thermal conductivity by a factor 5, and measuring a single crystal from the same batch, but with a larger diameter (10 times) increases by another factor three the thermal conductivity. Even if the thermal conductivity increase is less than the ratio of the crystal smaller dimensions, it is perfectly consistent with heat transport by ballistic phonons limited by the crystal size (or crystal imperfections). Note also that our results are consistent with the T^3 law deduced from "high temperature data" (T>3K) on a sample with intermediate diameter (2 mm) of [Slack & Oliver, 1971]. This thermal conductivity is also almost insensitive to magnetic field, again in agreement with a phonon-driven heat transport.

So, in this material, there is a strong decoupling between specific heat, governed by magnetic properties, and thermal transport, governed by phonons. This is a general feature of systems where local degrees of freedom (here, the magnetism of the Yb ions) yield the main contribution to specific heat. In this particular case, it implies that if the magnetocaloric effect is essentially the same for polycrystalline and single crystalline materials, at the same time, the thermal conductivity can vary by more than one order of magnitude between the different samples (see figure 3). Moreover, to further validate the use of this material for ADR applications, one should both take account of the low thermal conductivity (controlled by the phonons), leading to long heat diffusion times (see the work on the thermal bus described below), but also the diverging relaxation times (of the magnetic ions) below 0.3K, as noticed already by [Filippi et al, 1980]: this control also the cooling time of the material itself, independently from its geometry.

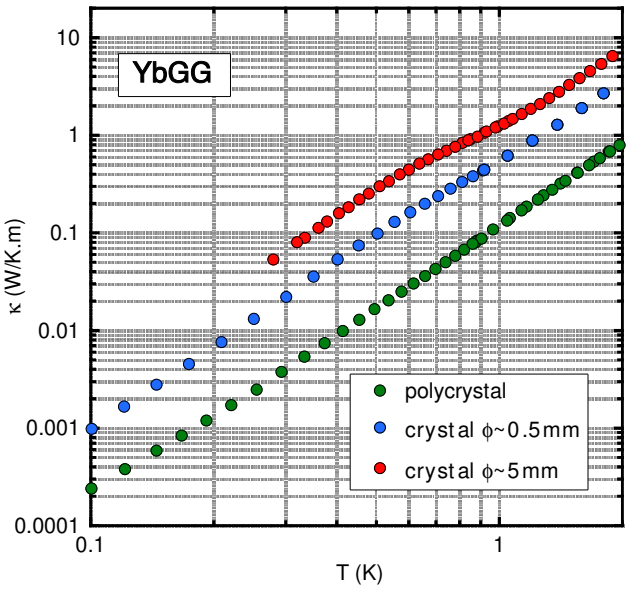

Figure 3 – Thermal conductivity of YbGG between 0.1 and 2K, for a polycrystalline sample, and two single crystals of different diameters: both the T^3 temperature dependence and the size-dependence point to a thermal transport governed by ballistic phonons (mean free path controlled by the crystal size).

In what follows, all presented results have been obtained on a large scale pill (400 g, 51.6 cm^3) made of polycrystalline material, with a copper thermal bus.

3. Characterization of a complete pill

Test bench and measurements method

For large scale characterization, a demonstrator model previously described [Brasiliano et al, 2016] has been used. It consists of three ADR stages in series. This is a modular prototype, allowing testing, comparing and characterizing different pills and materials.

The three ADR stages are connected in series by gas-gap heat switches such as described in [Duband et al, 1995].

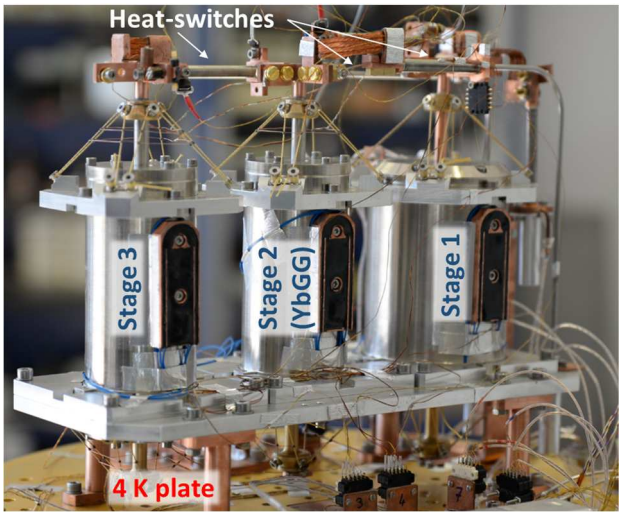

Figure 4 – Three stage ADR used for the demonstration.

An important parameter for the use of the pill is the thermal coupling between the thermal bus and the core of the material. For these measurements, the polycrystalline material has been glued, using stycast, to a copper surface.

Measurements of this coupling have been done based on a method previously described [Brasiliano et al, 2016] and shown schematically in figure 5. A heat pulse is applied to the thermal bus and its temperature is recorded over time. The thermal decoupling is obtained as the difference between the maximum temperature of the peak and the temperature reached once the peak load is stopped. This thermal decoupling comprises the thermal gradient in the copper part, the thermal decoupling at the interface copper/material, and part of the thermal gradient inside the material itself.

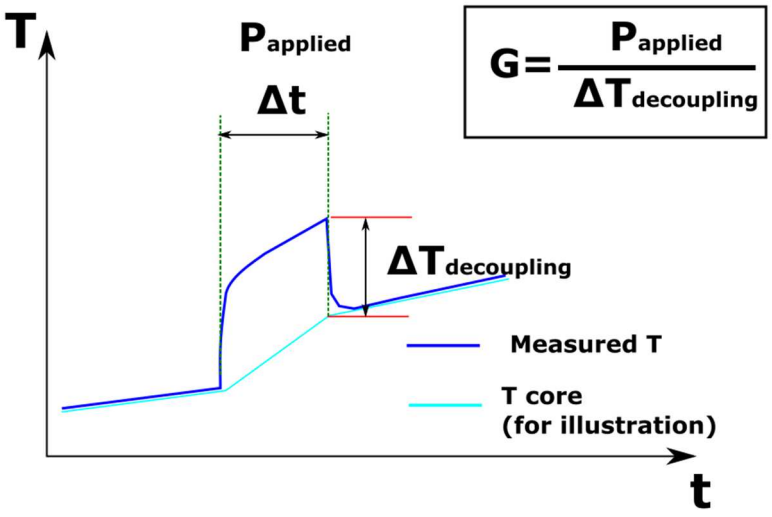

Figure 5 – Typical temperature profile obtained during the measurements of the pill thermal conductivity.

The results of these measurements are presented in figure 6. The data fits well with a second order power curve, which is consistent with a total thermal coupling composed by cooper (~T), thermal boundary and material (~T^3) conductivities. The measured thermal conductivity is large enough to accommodate most of the heat flux anticipated in the future developments. For high power application, the thermal coupling could be improved with a dedicated work on the thermal bus, for example increasing the section of the thermal bus itself and of the contact surface with the material.

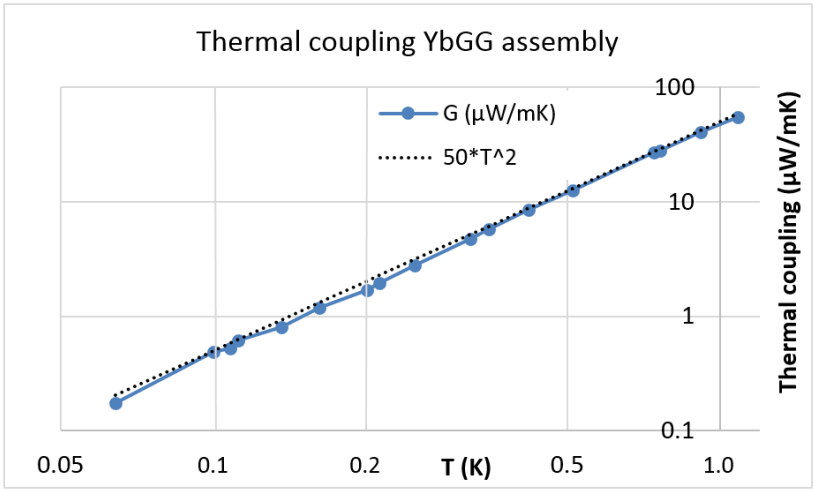

Figure 6 – Thermal coupling of the YbGG assembly

Entropy measurements

The entropy change versus magnetic field for fixed temperatures have been measured. Here the main goal is to validate the potential of this material in a representative experiment. This measurement is done by applying heat (through a heater) to the pill while regulating its temperature and by controlling the demagnetization rate. The magnetic current is recorded as function of the time and the mean magnetic field is directly deduced from the current. According to our simulations, the magnetic field over the pill is expected to variate of ± 5% around the mean magnetic field. Considering the calibration of the field versus current relationship, an error of up to 5% could be expected from the average value of B to its estimated value. In addition, there is a temperature gradient between the core of the material and the thermal interface due to the applied power. This gradient is taken into account on the presented results considering the pill thermal coupling measurements presented in figure 6. The energy is experimentally determined from the power applied and takes into account the estimated heat losses. These losses have been experimentally evaluated using a method described on a previous paper [Brasiliano et al, 2016]. The applied power was chosen to represent at least 10 times the value of the measured losses in order to increase the accuracy of the measurements.

Measurements have been done at temperatures of 100 mK, 150 mK, 200 mK, 400 mK, 800 mK, 1 K, 1.2 K, 2.0 K and 3.0 K. Some of those measurements are presented in figure 7 and compared to the calculations based on the free ion model. It is worth noting from figures 2 and 7 that this model reproduces the zero-field entropy within a few percent while underestimating the entropy change at constant temperature. It is therefore conservative to use this model to deduce the entropy.

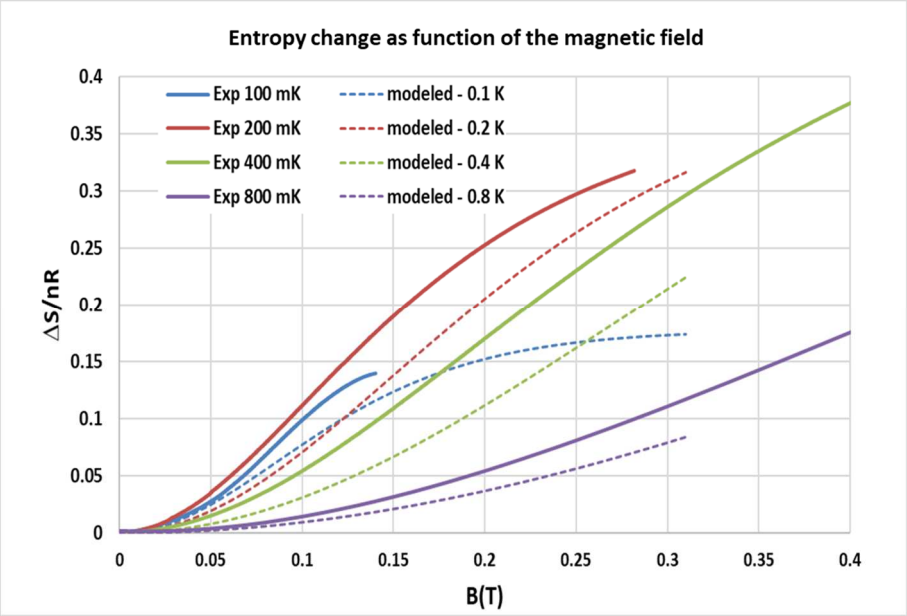

Figure 7 – Experimental and modeled entropy change for different temperatures.

4. Comparison with other materials and application

For the LiteBIRD mission mentioned in the introduction, an ADR cooler providing cooling power at 300 mK on the order of 20 to 50 µW and with an interface at 1.75 K is being discussed. Based on this material, we propose the design of a continuous cooling at 300 mK based on a two-stage configuration. This series configuration has been well described by [Shirron et al, 2000]. More data on the specific configuration will be described in [Duval et al, 2019]. It is based on a volume of material smaller than the one described in this paper meaning that the manufacturing process will be simplified. The typical volume of the stages is on the order of 30 cm^3 each. This two-stage continuous cooler can easily be completed using a third one-shot stage providing 50 or 100 mK for tens of hours depending on the mission requirements.

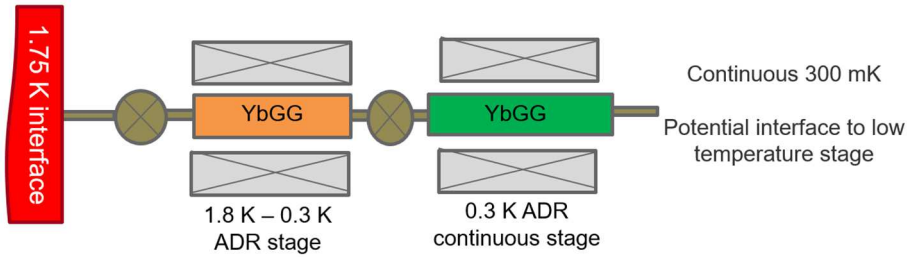

Figure 8 – Scheme of a 300 mK double ADR cooler.

The mass of an ADR stage is roughly proportional to the magnetic field required and the active volume of its material. The requirements for magnetic shielding have also a strong impact and we consider this effect to be similar for all considered cases.

To compare several materials, it is therefore possible to define a figure of merit given by BV, the maximum magnetic field times the volume of material. The total stage mass is roughly proportional to this quantity BV. To give an indication of the actual mass, a value of about 1.9 kg [Duval et al, 2019] is estimated for the case 1.75 K to 300 mK with 50 µW cooling power.

To reach temperatures lower than 500 mK, the typical material used for space application is chromic potassium alum (CPA). In figure 9, a comparison is made between CPA and YbGG. For CPA, for simplicity, only the free ion model is used based on values from the literature. No internal field is used giving therefore optimistic values. Other materials such as Gadolinium Gallium Garnet or Gadolinium Lithium Fluoride are not presented because 300 mK cooling could not be reached.

The advantage of YbGG is emphasized in figure 9: its figure of merit BV, for a stage recycling at 1.75 K, is significantly better than CPA's for a cold temperature above 200 mK. More specifically for the 1.75 K to 300 mK temperature range that is of particular interest for us, the use of YbGG is therefore very advantageous. The ratio of BV for YbGG relative to CPA is a factor of 1/3, which translates roughly to a reduction in mass by a factor 3.

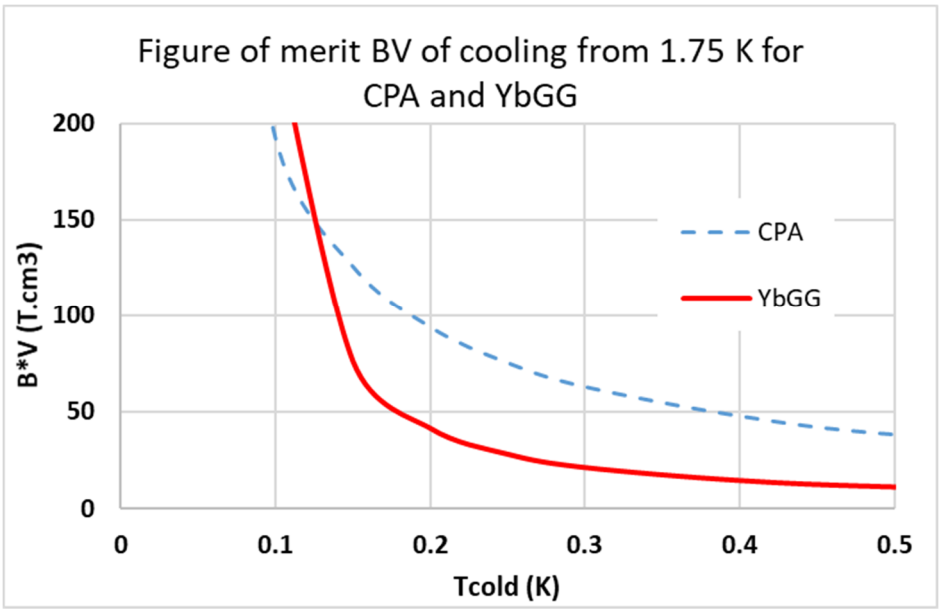

Figure 9 – Figure of merit necessary to obtain 180 mJ (50 µW, 1 hour) of cooling at a set temperature, from a 1.75 K interface.

5. Conclusion

Ytterbium Gallium Garnet is a very good candidate for space cryogenics ADRs. It is particularly well adapted for the 2 K – 200 mK temperature range.

In this paper, YbGG magnetocaloric properties are presented. A simple model of free ion has been proposed that fits the experimental data. It has been adjusted to fit heat capacity measurements for temperatures as low as 200 mK. There are still differences between the model and the experimental data, especially for the measurements of entropy change, suggesting that this frustrated material requires a more developed model if increased accuracy is required.

Finally, an example of cooler for which this material is particularly well suited is presented, which demonstrates a reduction by nearly a factor of 3 in mass compared to a cooler using conventional magnetocaloric material.

6. Acknowledgement

The authors would like to thank Jean-Louis Durand for the creativity in the experimental work, and the effort in providing accurate measurements. We also thank Daniel Braithwaite for heat capacity measurements made using a Quantum Design PPMS at PHELIQS. This work has been done with the partial support of CNES PhD program, including R&T R-S13/SU-002-080, DSM Energie program and CEA PTC (Programme Transverse “matériaux et procédé” -2016-2018).

7. References

1. [Wikus et al, 2011] Wikus, P., G. Burghart, and E.I. Figueroa-Feliciano. « Optimum operating regimes of common paramagnetic refrigerants ». Cryogenics (2011).
2. [Brasiliano, 2017] « Etude et réalisation d'une ADR spatiale 4 K - 50 mK » PhD thesis, Grenoble Alpes University, 2017.
3. [Barcley and Steyert, 1982] Barclay, J. A. and Steyert, W. A., “Materials for magnetic refrigeration between 2 K and 20 K”, Cryogenics 22, 73 (1982).
4. [Filippi et al, 1980] Filippi, J., Lasjaunias, J. C., Hebral, B., Rossat-Mignod, J., and Tcheou, F., “Magnetic properties of ytterbium gallium garnet between 44 mK and 4 K” Journal of Physics C: Solid State Physics 13, 1277 (1980).
5. [Zhitomirsky , 2003] M. E. Zhitomirsky : “Enhanced magnetocaloric effect in frustrated magnets” Phys. Rev. B 67, 104421 (2003).
6. [Pobell, 2007] Pobell, F, “Matter and Methods at low temperatures”, Ed Springer, 3rd edition, 2007.
7. [Shirron, 2014] Shirron, P. J., “Applications of the magnetocaloric effect in single-stage, multi-stage and continuous adiabatic demagnetization refrigerators”, Cryogenics 62, 130 (2014).
8. [Slack et Oliver, 1971] Slack, Glen A. and Oliver, D. W., “Thermal Conductivity of Garnets and Phonon Scattering by Rare-Earth Ions”, Phys. Rev. B, 4, 592 (1971).
9. [Onn et al, 1967] Onn, D. G., Meyer, H., and Remeika, J. P., Phys. Rev. 156, 663 (1967).
10. [Brasiliano et al, 2016] Paixao Brasiliano, D. A., Duval, J. M., Luchier, N., D’Escrivan, S., and André, J., in Cryocoolers 19 (S. D. Miller, R. G. Ross, Jr., 2016) pp. 479 – 485.
11. [Duband et al, 1995] Duband, « A thermal switch for use at liquid helium temperature in space-borne cryogenic system » ICC, 1995.
12. [Shirron et al, 2000] Shirron, P. J., Canavan, E. R., DiPirro, M. J., Tuttle, J. G. and Yeager, C. J. "A multi-stage continuous-duty adiabatic demagnetization refrigerator." Advances in cryogenic engineering. Springer US, 2000. 1629-1638.
13. [Duval et al, 2019] Duval, JM., Attard, A., Brasilano, D. A. P. “Experimental results of ADR cooling tuned for operation at 50 mK or higher temperature” To be published and presented in Advances in Cryogenic Engineering, 2019.